



Slow pyrolysis of *Spirulina platensis* for the production of nitrogenous compounds and potential routes for their separation

K.C. Rocha^a, C.G. Alonso^a, W.G.O. Leal^b, E.L. Schultz^b, L.A. Andrade^{a,*}, I.C. Ostroski^a

^a Institute of Chemistry, Federal University of Goiás, CEP 74690-900 Goiânia, GO, Brazil

^b Embrapa Agroenergia, CEP 70770 901 Brasília, DF, Brazil

ARTICLE INFO

Keywords:

Fine chemistry
Bio-oil
Heterocyclic compounds
Extraction
Adsorption

ABSTRACT

The potential of microalgae *Spirulina platensis* to the production of nitrogenous compounds in liquid fraction by slow pyrolysis was evaluated. Aiming to identify the best condition which maximized liquid yield, the effects of operational conditions mass load, temperature, and heating rate were evaluated using Experimental Design and Response Surface Methodology techniques and optimized with Differential Evolution methodology. The composition of liquid fraction was analyzed by GC-MS and the effect of the same operational conditions in nitrogenous compounds formation was analyzed. The separation of nitrogenous compounds was evaluated by extraction and adsorption techniques. The results indicated that the heating rate significantly impacted both the liquid yield and the formation of the nitrogenous compounds. At optimal conditions, a maximum liquid yield of 64.59% was obtained. The extraction and adsorption processes showed to be promising routes for the purification of nitrogenous compounds, however, extraction was more selective to separate them.

1. Introduction

Investigations on the use of microalgae biomass have been growing in recent years due to its characteristics of high growth rates, even in non-potable waters, and also for being adaptable to climate change (Pourkarimi et al., 2019).

Among the possible biomass conversion routes, the pyrolysis process has been highlighted. Pyrolysis is the thermochemical decomposition of raw material that occurs in the absence or partial presence of oxygen and produces solid, liquid, and gas. It can be categorized into slow pyrolysis and fast pyrolysis based on the heating rates (Hu and Gholizadeh, 2019). Fast pyrolysis has been highlighted as a route for the generation of bio-oil rich in hydrocarbon while slow pyrolysis has been reported to not generate a high hydrocarbon content, due to a greater tendency to promote secondary reactions (Bridgwater and Bridge, 1991). In this context, *Spirulina platensis* is known as high protein biomass, and due to this factor, it may be unfavorable to processes whose objective is the generation of hydrocarbons (Hong et al., 2017).

The liquid fraction from biomass pyrolysis has been standing out as a potential product to replace transport fuels, especially when high amounts of hydrocarbons can be generated (Sharma et al., 2015). In this sense, the microalgae biomass has been studied as a feedstock for biofuel production (Simão et al., 2018). However, even with research in this area over the decades, there is no liquid fuel yet capable of

replacing those generated by fossil raw material (Fermoso et al., 2017).

An attractive alternative for the application of bio-oil that has still not yet been satisfactorily investigated is the generation of high added-value chemicals. Huang et al. (2017), for instance, studied microwave catalytic pyrolysis with microalgae to obtain nitrogenous compounds. The highest bio-oil yield was 48.8% at 500 °C, and the nitrogenous compounds found that have the highest aggregate values were indole and dodecamide. Maliutina et al. (2018) studied pressurized entrained-flow pyrolysis with microalgae and the main nitrogenous compounds found were indolizine, indole, and quinoline with 43.23% of maximum nitrogenous yield. Ma et al. (2019), studied fast pyrolysis with bamboo biomass (*Phyllostachys edulis*) doped with ammonia and obtained the maximum formation of nitrogenous compounds of 19.89% at 300 °C, with generation mainly of pyridines, pyrroles, and amines.

To obtain nitrogenous compounds with high added-value, after pyrolysis, separation process must be applied, since the bio-oil contains a blend of compounds. These compounds could be separated by adsorption. Li et al. (2019b), for instance, studied the adsorption of nitrogenous compounds from microalgae bio-oil by using activated carbon, activated silica gel, and Cu-zeolite Y. The authors observed that the adsorption capacity of nitrogenous compounds using activated carbon (18.06 mg of N g⁻¹) was higher than activated silica gel (7.28 mg of N g⁻¹) and Cu-zeolite Y (8.12 mg of N g⁻¹). Although it has stood out for its adsorption capacity, activated carbon was not selective

* Corresponding author.

E-mail address: laianealves@ufg.br (L.A. Andrade).

<https://doi.org/10.1016/j.biortech.2020.123709>

Received 5 May 2020; Received in revised form 15 June 2020; Accepted 16 June 2020

Available online 19 June 2020

0960-8524/ © 2020 Elsevier Ltd. All rights reserved.

because it also removed other compounds of interest from bio-oil when used as a fuel. [Bhadra and Jhung \(2020\)](#) investigated the use of metal-organic framework adsorbents (MIL-125 and UiO-66), with and without $-NH_2$ groups, and activated carbon to remove organo-nitrogen compounds from microalgae derived bio-oil. All adsorbents, including activated carbon, were shown to be able to remove organo-nitrogen compounds, however, the MIL-125 with $-NH_2$ was much more efficient. In both works, nitrogenous compounds were seen as contaminated and, therefore, the aim was to remove them for a possible application of bio-oil as fuel and no concern about separated the distinct classes of nitrogenous compound or even purification of this compounds was highlighted in these studies.

Extraction is another possibility for the separation of bio-oil compounds. [Fan et al. \(2019\)](#) showed the extraction efficiency of nitrogenous compounds (quinoline, indole, and carbazole) from the diesel model with ionic liquids. [Salleh et al. \(2017\)](#) also demonstrated good results on nitrogenous compounds (pyrrole, indoline, pyridine, and quinoline) extraction with the ionic liquid 1-ethyl-3-methylimidazolium methanesulfonate. [Han et al. \(2013\)](#), in turn, studied the extraction of basic nitrogenous compounds from Fushun shale oil with acid phosphoric (A), acid phosphoric and acid sulfuric (A:B), acid phosphoric and acetic acid (A:C), methanol-acidic and acid sulfuric (D:B), and formic acid and acetic acid (E:C). They indicated good extraction with all solvents, but with A:B and A showing the best results, 97,43% and 96,04% of basic nitrogenous compounds, respectively. The denitrogenation process using phosphoric acid was also described as successful by [Smith \(1981\)](#), with shale oil samples. It has been demonstrated in the literature that the pyrolysis product yields and bio-oil quality depend on operational parameters such as temperature, heating rate, mass load, among others ([Fanghua et al., 2019](#)). Even, the effects of operational parameters on the yield and quality of the product in a pyrolysis process have been investigated by some authors, most of them are focus on fast pyrolysis to the production of fuels. The study on the influence of operational parameters in the slow pyrolysis process with the objective of forming chemicals of commercial interest, as well as the routes for separated these compounds is remained poorly explored in the literature.

Therefore, the aim of this study was to evaluate the operational conditions mass load, heating rate, and temperature on liquid yield and on the production of nitrogenous compounds via slow pyrolysis using *Spirulina platensis*. Besides, the extraction and adsorption processes were evaluated as possible routes for the separation of nitrogenous compounds to be used as high added value chemicals. An optimization study was also performed to identify the conditions that lead to the maximization of the liquid yield.

2. Materials and methods

2.1. Biomass characterization

The microalgae used in pyrolysis experiments was *Spirulina platensis* purchased from Brasil-Vital Company (Anápolis, Goiás, Brazil). At first, the biomass was ground and sieved, and the particle sizes smaller than 0.12 mm were used for the tests. The biomass was dried at 60 °C for 36 h, the time necessary to achieve constant weight. The final moisture of *Spirulina* was 6.90%. The microalgae batch used in this work is the same used by [Barbosa et al. \(2020\)](#) in which a more detailed characterization can be found. According to the authors, the amount of protein and nitrogen were 52.90 ± 0.87 (wt %) and 9.64 (wt %), respectively.

2.2. Pyrolysis process

Pyrolysis experiments were carried out in a batch reactor. The reactor was placed inside a muffle furnace connected to a condensation system and a vacuum pump. The condensation system was composed

by a set of condensation traps immersed in ice in order to capture the liquids, and the vacuum pump was used to improve in the flow of gas downstream of the reactor and avoid the presence of oxygen in the reactor.

2.3. Experimental design

The central composite design (CCD) was used to evaluate the effect and interactions of the variables mass load (M), temperature (T), and heating rate (HTR) on product yields and distribution of the main products (nitrogenous, oxygenated, and hydrocarbons) during pyrolysis. Moreover, the Response Surface Methodology (RSM) was used to evaluate the profiles of studied variables on the liquid yield response.

The CCD approach allows analyzing the influence of the process variables on the response with a smaller number of experiments, which reduces reagent consumption and laboratory work. It consists of three parts: factorial design $2^k (\pm 1)$, axial points ($\pm \alpha$), and center points ([Ataefard and Saeb, 2015](#)). The central point repetitions permit evaluated the experimental errors and the reproducibility of the data.

The independent variables M, T, and HTR are represented by the coded forms x_1 , x_2 , and x_3 , according to equations (1)–(3), respectively. The ranges of the variables M, T, and HTR were 1.98 to 5.52 g, 309 to 592 °C and 1.7 to 10.2 °C min⁻¹, respectively, which were determined according to the capacity of the equipment.

$$x_1 = \frac{M(g) - 3.75}{1.25} \quad (1)$$

$$x_2 = \frac{T(^{\circ}C) - 450}{100} \quad (2)$$

$$x_3 = \frac{HTR(^{\circ}C \text{ min}^{-1}) - 6.0}{3.0} \quad (3)$$

The experimental design based on the CCD for three variables presented 18 configurations of pyrolysis operations divided in 8 factorial points, 6 axial points ($\alpha = \pm 1.41$), and 4 repetitions of central point ([Table 1](#)). The analysis of variance (ANOVA), through p-value and lack of fit, was performed to check if the results were meaningful ([Ataefard et al., 2016](#); [Hosseinneshad et al., 2017](#)). Each variable was evaluated considering its influence on the response with a 90% confidence level, $p (< 0.10)$. The results were analyzed using the software R version 3.6.1.

2.4. Yields of pyrolysis products and optimization process

The yields of pyrolysis products were determined by gravimetric analysis. The amount of liquid and solids produced during pyrolysis was

Table 1
Central Composite design conditions for pyrolysis of *Spirulina platensis*.

Experiments	x_1	x_2	x_3	M (g)	T (°C)	HTR (°C min ⁻¹)
1	-1.00	-1.00	-1.00	2.50	350	3.0
2	-1.00	-1.00	1.00	2.50	350	9.0
3	-1.00	1.00	-1.00	2.50	550	3.0
4	-1.00	1.00	1.00	2.50	550	9.0
5	1.00	-1.00	-1.00	5.00	350	3.0
6	1.00	-1.00	1.00	5.00	350	9.0
7	1.00	1.00	-1.00	5.00	550	3.0
8	1.00	1.00	1.00	5.00	550	9.0
9	-1.41	0.00	0.00	1.98	450	6.0
10	1.41	0.00	0.00	5.52	450	6.0
11	0.00	-1.41	0.00	3.75	309	6.0
12	0.00	1.41	0.00	3.75	591	6.0
13	0.00	0.00	-1.41	3.75	450	1.7
14	0.00	0.00	1.41	3.75	450	10.2
15	0.00	0.00	0.00	3.75	450	6.0
16	0.00	0.00	0.00	3.75	450	6.0
17	0.00	0.00	0.00	3.75	450	6.0
18	0.00	0.00	0.00	3.75	450	6.0

divided by the initial amount of biomass fed into the reactor, and the results were expressed as a percentage. The yield of gas was determined by mass balance. Through the experimental results, the empirical equations of second-order that predict the product yields were obtained. The insignificant terms were eliminated and the reduced form of the equations was used in order to increase the reliability and precision of the model's predictions.

Aiming to maximize the liquid yield, an optimization study was performed. In this sense, the reduced quadratic model from the CCD combined with the Differential Evolution (DE) algorithm methodology was adopted. DE is a population-based optimizer inspired on Darwin's theory of evolution. The computational code was an adapted version from the version developed by [Vieira et al. \(2011\)](#), implemented in Scilab 6.0.2 software. The DE parameters used were 50 individuals, 250 generations, 0.8 scale factor (F), 0.8 crossover probability (Cr), and classical method DE/rand/1/bin. The number of generations was used as a criterion for interrupting the procedure. The restriction that the other yields were higher than zero was adopted.

2.5. Gas chromatography–mass spectrometry (GC–MS) analysis.

Gas chromatography–mass spectrometry analysis was used to identify the main chemical compounds in bio-oil samples. A semi-quantitative analysis of the chemical compounds in the bio-oil was performed based on the intensities of the relative peaks. This is possible due the fact that, the chromatographic peak area is linearly related to its quantity, and the relative peak areas are considered to be linearly related to the content. Thus, the peak area percentage of the compounds can be compared in order to observe the change in their relative contents in the pyrolysis vapors ([Qiang et al., 2009](#)). Thus, for data treatment, the variations in the contents of the compounds with the studied parameters were analyzed using the area percentages of their respective peaks. The products were classified as nitrogenated, oxygenated and hydrocarbons compounds using the sum of percentages of the peak areas related to each group.

The bio-oil was diluted in approximately 60–70% by weight of dichloromethane and carefully homogenized. GC–MS analyses were performed using a 60 cm Rtx-1701 GC 195 column (60 m × 0.25 mm in diameter and 0.25 μm film thickness). The linear velocity was fixed at 25.6 cm s⁻¹ and the purge flow at 3 ml min⁻¹. The initial temperature of the GC furnace was adjusted to 45 °C and maintained for 4 min. Then it was increased to 280 °C at a heating rate of 3 °C min⁻¹. The injection temperature was 250 °C and the chromatography/spectrometer interface temperature was 275 °C. The assignments for the main peaks were made using retention time data and the library from the National Institute of Standards and Technology (NIST version 05). The compounds with a similarity index higher than 80% have been identified.

2.6. Fourier transform infrared (FTIR)

The FTIR spectra were also performed on bio-oil samples to determine the main components, according to the peaks of the functional groups. The analyses were performed on a PerkinElmer spectrophotometer, model Spectrum 400, with wavelength range 4000–400 cm⁻¹ and 32 scans. The samples were analysed using the KBr disk method. A graphic software was used to correct its baselines.

2.7. Extraction

The sample was prepared by adding 2 g of liquid fraction, solubilized in dichloromethane, and 0.06 g of phosphoric acid (85%). After that, the sample was stirred for 20 min and then placed for 4 h of decantation in a separatory funnel. The two phases were separated and analyzed by FTIR and GC–MS methods. These conditions were based on ([Han et al., 2013](#)) who had a good results in removal of nitrogenous compounds from Fushun shale oil.

Table 2

ANOVA table assigned to the quadratic reduced model relating to liquid yield response.

Source	Sum of Squares	Df	Mean Square	F value	p-value	
Model	0.1214	5	0.0243	26.0078	< 0.0001	significant
M	0.0044	1	0.0044	4.6704	0.0516	
T	0.0615	1	0.0615	65.8689	< 0.0001	
T ²	0.0235	1	0.0235	25.1471	0.0003	
HTR ²	0.0244	1	0.0244	26.1010	0.0002	
M × T	0.0077	1	0.0077	8.2519	0.0140	
Residual	0.0112	12	0.0009			
Lack of Fit	0.0102	9	0.0011	3.6079	0.1595	insignificant
Pure Error	0.0009	3	0.0003			
Cor total	0.1326	17				
Std. Dev.	0.0883		R ²	0.9155		
Mean	0.5175		Adj. R ²	0.8803		

2.8. Adsorption

The adsorption experiment was carried out with coconut shell activated carbon chemically modified with sulfuric acid (SAAC), previously characterized by our group ([Ferreira et al., 2019](#)). In that study, it was observed that SAAC proved to be a promising material for adsorption of nitrogenous compounds in oil fractions. Considering the similarity of bio-oil to oil fractions, activated carbon was chosen as an adsorbent to be tested in this work.

The experiment was carried out in duplicate by using a rotary shaker. In an Erlenmeyer flask was added 0.5 g of activated carbon and 5 ml of bio-oil solubilized in dichloromethane and then placed under stirring for 24 h at 130 rpm and 25 °C. After that, the solution was filtered and the liquid phase analyzed by GC–MS.

3. Results and discussion

3.1. Effect of multivariable system in pyrolysis liquid yield

[Table 2](#) shows the ANOVA results for the reduced quadratic model obtained for liquid yield, in which the p-value of the model is satisfactorily meaningful (p < 0.0001). The p-value of the “lack-of-fit” (0.159) replies to the reliability of the model and R² value of 0.9155 indicated that 91.55% of variability of the data can be expressed by the model, which is reasonably adequate. The results of ANOVA for yields of solid and gas are given in [Supplementary material](#). The reduced quadratic model predicting the yields of liquid (RL), solid (RS) and, gas (RG) as a function of the independent variables mass (x₁), temperature (x₂), and heating rate (x₃) are given in Eqs. (4)–(6).

$$RL = 0.517 + 0.019x_1 + 0.071x_2 - 0.054x_2^2 + 0.055x_3^2 - 0.0310x_1x_2 \quad (4)$$

$$RS = 0.330 - 0.089x_2 + 0.054x_2^2 + 0.009x_1x_3 - 0.018x_2x_3 \quad (5)$$

$$RG = 0.155 - 0.020x_1 + 0.018x_2 - 0.058x_3^2 + 0.032x_1x_2 \quad (6)$$

The statistical analysis indicated random, independent, and small residues with normal distribution (mean of zero and constant variance), as can be seen in the distribution histogram found in the [Supplementary material](#).

3.1.1. Interactions between operations parameters on the liquid yields

As the liquid is a source of high-value chemicals, it is considered an interesting fraction of pyrolysis. Thus, the effects of mass load (M – x₁), temperature (T – x₂), and heating rate (HTR – x₃) on the liquid yield (fraction typically composed of water and bio-oil) were investigated using RSM.

[Fig. 1a](#) shows the effects of independent variables mass load and temperature on the liquid yield, with the heating rate at the central level (x₃ = 0). The [Fig. 1a](#) presents that the temperature had a

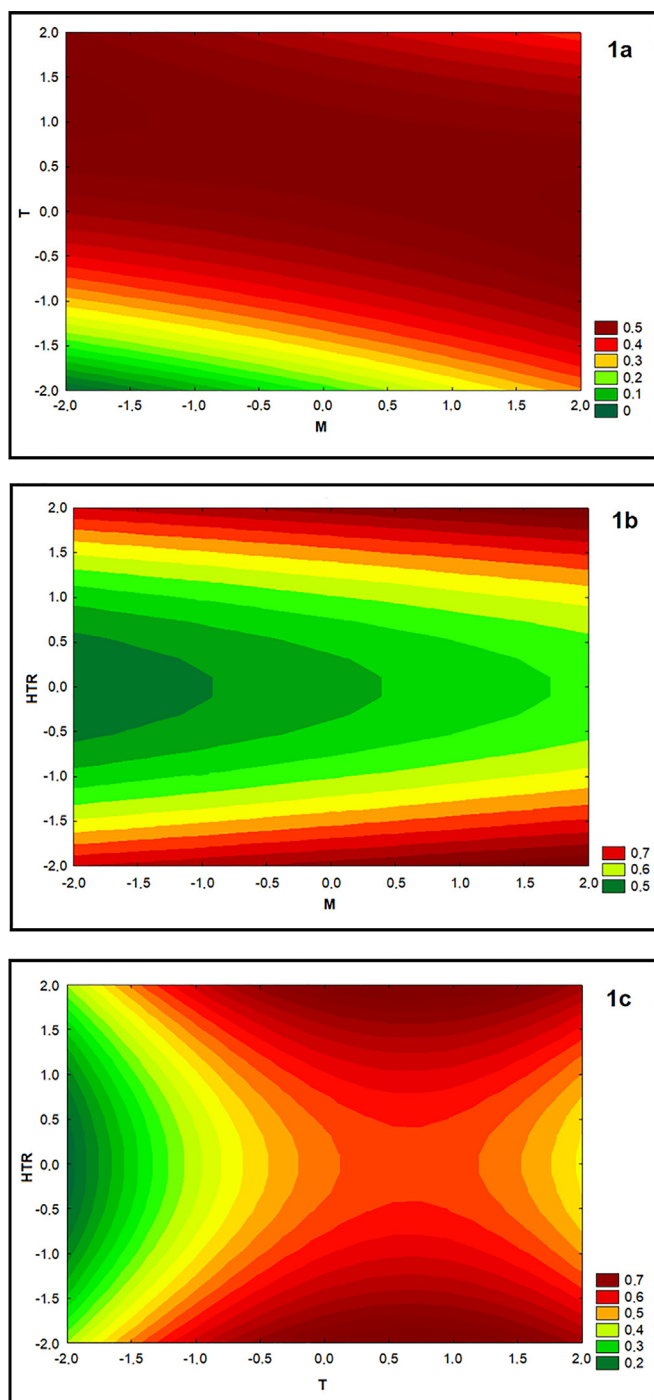


Fig. 1. 1a Interaction between mass load and temperature on liquid yield. 1b Interaction between mass load and heating rates on liquid yield. 1c Interaction between temperature and heating rates on liquid yield.

significant influence on liquid formation, and the range close to the central level showed higher yields. The curvature indicates a tendency for the yield to decrease with increasing or decreasing temperature. In the case of higher temperatures, pyrolysis possibly became more favorable to the formation of gases. On the other hand, at lower temperatures, there is probably not enough energy for the complete degradation of biomass and, consequently, there is an increase in the formation of solids. The effect of temperature observed in this work corresponds to other ones presented in the literature. Hu et al. (2013) performed pyrolysis with blue-green algae in a fixed-bed reactor at heating rate of $40\text{ }^{\circ}\text{C min}^{-1}$ and found that the production of bio-oil

increased from 26.66 to 54.97% with an increase in temperature from 300 to 500 $^{\circ}\text{C}$ and decrease to 38.36% at 700 $^{\circ}\text{C}$. Yang et al. (2014) also identified the influence of temperature on product formation in the pyrolysis of with microalgae *Spirulina* using a fixed bed reactor, and observed the highest liquid yield (35.05%) at 450 $^{\circ}\text{C}$. Huang et al. (2017) studied the effects of temperature (350–650 $^{\circ}\text{C}$) associated with activated carbon and Fe_3O_4 catalysts on the yield of products in microwave pyrolysis using the microalgae *Chlorella* and *Spirulina* as biomass. For both microalgae, the highest liquid yields were in the temperature range between 450 and 550 $^{\circ}\text{C}$. The behavior found in this work and reported by other authors with respect to temperature is common to biomass pyrolysis processes. However, the combinations effects of operational parameters and how these parameters can influence the process performance remains poorly explored. In this sense, although Eq. (4) indicates that the mass load (x_1) was also a significant effect for the liquid yield, Fig. 1a highlights that this effect was less pronounced when compared to the effect of temperature. Two opposite scenarios can be observed concerning biomass load when not ideal temperatures for pyrolysis process were used ($x_2 \neq 0$). In the first, it was observed that for high temperatures the smaller amounts of mass load were slightly more favorable to increase the liquid yield. Conversely, the second scenario highlights that when lower temperatures were carried out higher biomass amounts were more favorable to increase the liquid yield. Additionally, it was visible that the biomass mass effect becomes more pronounced when lowers temperatures were applied. Possibly, for the first scenario, the smaller amount of biomass could favor a rapid degradation of the biomass, preventing the vapors from spending a longer residence time inside the reactor which at high temperature can favor the cracking reactions which would favor the formation of gases (Guedes et al., 2018). The use of less biomass amounts could be interesting when it comes to the intensification of processes in a system of continuous operation mode. In this case, smaller amounts of biomass could be fed into the reactor and quickly converted to, mainly, the liquid formation. However, the quality of bio-oil generated in such conditions must be carefully analyzed to see if the desired chemical species were formed under these conditions. For the second scenario (lower temperatures) the higher biomass amount proved to be favorable to the increase in liquid yield. At these conditions, where less energy for the reaction is available, the greater amounts of biomass can be favor to increase the vapors' residence time due to biomass represent a solid barrier during its degradation, hindering the release of vapors (Andrade et al., 2018). This barrier to vapor release possibly affected more significantly the release of the lighter (non-condensable) gases in the reaction zone and possibly favored the interaction between molecules promoting reactions such as Maillard, which happen at lower temperatures comparing with pyrolysis temperature (400–500 $^{\circ}\text{C}$) (Guo et al., 2017). The Maillard reaction occurs at temperatures below 350 $^{\circ}\text{C}$, indicating that it occurred during the heating of the biomass. Whereas the heating rates used were low (1.7 to 10.4 $^{\circ}\text{C min}^{-1}$), Maillard's reaction might have been favored throughout the pyrolysis process. Maillard reaction is the reaction of amino compounds with aldehydes or ketones associated with the formation of browning polymeric materials (Wang et al., 2017). These two opposite scenarios show the different dynamics in terms of reaction routes that can happen depending on the operational conditions of the process, which will impact directly the product quality in the liquid fraction.

Fig. 1b shows the effects of mass load and heating rate on the liquid yield, with the temperature at the central level ($x_2 = 0$). It can see that there are two favorable scenarios for increasing liquid yields, when the heating rate is high or low. Probably, the lowest rates contributed to a better degradation in the raw material, considering that the biomass residence time of biomass inside the reactor for these conditions was higher. It must be emphasized that, according to the literature, low heating rates induce a long residence time for vapors within the reaction zone and consequently favor secondary reactions which decrease

the quality of bio-oil, when fuel production is the goal (high hydrocarbon concentration) (Fanghua et al., 2019). On the other hand, higher heating rates reduce the limitation of mass and heat transfer, favoring the rapid fragmentation of the particles and decreasing the time available for the formation of secondary reactions, increasing the generation of liquids, when adequate pyrolysis temperature (≈ 500 °C) was used (Akhtar and Noraishah, 2012).

The mass load showed less pronounced influence when compared to the heating rate, however, the higher mass load was slightly more favorable to the increase in the liquid yield. Probably, as the mass increases, the more difficult it is to release vapors, especially the lighter fractions, due to the physical barrier imposed by biomass. In this sense, polymerization reactions of these molecules, especially via the Maillard reaction, could still be favored with the temperature condition at the central point (450 °C) slightly favoring the formation of heavier fractions (condensable gases or solid fraction).

Fig. 1c shows the effects of temperature and heating rate on the liquid yield, with the mass load at the central level ($x_1 = 0$). In agreement with the other surfaces, both high and low rates are favorable to the liquid yield when the temperature is close to the central level. As discussed earlier, low rates are not a favorable scenario to produce quality bio-oil when fuel production is concerned, since they favor secondary reactions during the process. However, these secondary reactions can be interesting to generate valuable nitrogenated molecules via Maillard or via surfactant synthesis reaction which promotes a combination of molecules from the breakdown of carbohydrates and proteins, and lipids and proteins, respectively. These reactions, typically already occur in the pyrolysis process of microalgae; however, possibly the increase in residence time could favor their occurrence due to a longer time of the molecules released during the biomass degradation in the reaction zone. The Maillard reactions, typically, are responsible for generating N-heterocyclic compounds such as pyrazol, pyrrole, piperazine, piperidine, azetidine, pyrrolidine, indole, pyrazine, pyrimidin, pyridine, and so on, while surfactant synthesis reaction is evidenced by the presence of amides and amines in the bio-crude (Wang et al., 2017).

3.2. Optimization

The results of the optimization study found the following ideal operating conditions: mass = 1.98 g, temperature = 556 °C, and heating rate = 10.24 °C min^{-1} . The calculated yields were 66.04%, 25.15%, and 3.90% for liquid, solid, and gas, respectively. A confirmatory experiment was performed at the optimum condition, and the results are 64.59% liquid, 28.38% solid, and 7.09% gas. The experimental and predicted responses are in good agreement, with a relative error of less than 10% to liquid yield. Besides, the experimental result of liquid yield obtained under the optimal conditions is higher than all those obtained in the CCD data.

The results obtained in the optimization model are in agreement with the results obtained by the response surface in which show less biomass, temperatures close to 550 °C, and high or low heating rates resulting in higher liquid yield. Thus, the parameters obtained by the optimization are within the expected limit and can be considered acceptable.

The maximum yield of liquid obtained during the pyrolysis in this work was higher than some works reported on literature for *Spirulina platensis*. Jena and Das (2011) carried out a pyrolysis study to produce bio-oil using *Spirulina platensis* the highest liquid yield of 46.6% was obtained with a temperature of 500 °C and a heating rate of 7.0 °C min^{-1} . Hong et al. (2017) performed microwave pyrolysis of *Spirulina platensis* reaching at best condition (550 °C and 40 °C min^{-1}) around 26% of liquid yield and the gas as the majority product. Huang et al. (2017) also carried out a microwave pyrolysis of *Spirulina* sp. and obtained 48.4% of liquid yield at 500 °C in a presence of Fe_3O_4 . Barbosa et al. (2020) conducted an optimization study of catalytic pyrolysis of

Table 3

Relative percentages of hydrocarbon, oxygenated, and nitrogenous compounds.

Experiments	Liquid yields	Hydrocarbon	Oxygenated	Nitrogenous
1	38.40	0.00	13.25	55.25
2	42.46	3.05	26.11	63.31
3	61.60	4.20	19.70	68.06
4	57.42	4.02	36.03	46.22
5	55.52	1.82	15.72	66.88
6	44.78	1.69	27.92	63.53
7	56.17	0.00	0.00	88.82
8	57.46	0.00	4.30	77.88
9	46.66	0.00	16.86	83.14
10	52.90	1.70	29.75	54.46
11	28.80	2.20	23.45	63.66
12	53.13	10.00	18.30	63.96
13	64.07	0.00	0.00	90.64
14	61.60	1.57	27.11	50.94
15	53.47	2.82	22.67	50.41
16	51.73	0.00	25.49	52.25
17	54.66	0.00	0.00	56.84
18	50.67	0.00	22.56	60.61
Optimization point	64.59	5.52	14.35	73.73

Spirulina platensis under 500 °C and 2.5 °C s^{-1} reaching a maximum liquid yield of 35%. This fact may suggest that even low heating rates are capable of generating significant amounts of liquid product in the case of the *Spirulina* microalgae.

Additionally, it is noted that operational differences in the processes led to different yields, which reinforces that the operational parameters (reported in this study and others) must be evaluated together to reach optimized conditions.

3.3. Gas chromatography–mass spectrometry (GC–MS) analysis

The results of the GC–MS analyses show the formation of diverse organic compounds in the bio-oil under the various operational conditions evaluated. Table 3 presents the results of liquid yields (%) and relative percentages of hydrocarbon, oxygenated, and nitrogenous compounds present in the bio-oil for each test of the CCD and the optimization point.

As can be seen, all tests obtained higher formations of nitrogenous compounds. The large amounts of these compounds are related to the raw material, *Spirulina platensis* microalgae, which has a high protein content in its composition (up to 70%). Besides, the Maillard reaction, an interaction between proteins and carbohydrates, may have occurred, which causes an increase in the formation of heterocyclic nitrogenous compounds (Wang et al., 2017).

The tests that obtained 0% of hydrocarbon and oxygenated compounds do not necessarily indicate the non-presence of these compounds, but the non-identification by the method. This occurs because the identification of the compounds in the GC–MS analysis is carried out with an 80% similarity.

Table 3 also shows that the optimization point, as previously discussed, obtained the highest liquid yield, however, it was not the best condition for the generation of nitrogenous compounds. In the representative fraction of the liquid yield, the highest concentration of nitrogenous compounds (90.64% relative percentage area) was observed in experiment 13 ($M = 3.75$ g, $T = 450$ °C, and $T_x = 1.7$ °C min^{-1}). Although these experiments did not have similar operating conditions, the liquid yield achieved was similarly high (64.07%). Probably, the operational conditions of experiment 13 benefited Maillard reactions, due to slow degradation of biomass (lowest heating rate), forming more nitrogen compounds, but without interfering significantly in the liquid yield. This fact indicated that quality of bio-oil was also influenced by the operating conditions used in the process. Observing the tests carried out at the axial points (tests 9–14) the operation conditions of mass load and the heating rate at the

axial points showed to be meaningful for nitrogenous compound formation. Smaller amounts of mass (test 9) or lower heating rates (test 13), that is, conditions which provided a longer residence time of biomass inside the reactor, led to a higher formation of nitrogenous compounds, reinforcing the occurrence of the Maillard reaction.

3.4. Potential routes to separate the nitrogenous compounds

GC–MS analyses identified large amounts of compounds in the bio-oil, especially nitrogenous compounds (46.22–90.64%). Aiming to investigate possible routes for the purification of these products, studies on their separation by extraction and adsorption were carried out, with the bio-oil generated under the conditions of the experiment 13, which provide the highest concentration of these compounds and significantly liquid yield.

3.4.1. Extraction

The chemically active extraction technic was used. This technique is used to separate organic compounds soluble in the same solvent by adding a new solvent. After extraction, the light phase was analyzed by the GC–MS technique.

The results showed that the extraction was effective and selective for separation of nitrogenous compounds since some compounds were preferably in the light phase and others in the heavy phase (Fig. 2a). Additionally, it was possible to observe a slight increase of the compounds which remained in the light phase after the extraction (Fig. 2a), indicating that they were concentrated in the light phase of extraction (dichloromethane). Similarly to this work, Han et al. (2013) studied extraction with phosphoric acid from Fushun shale oil and showed good results for nitrogen removal.

According to GC–MS analysis of bio-oil samples before and after extraction, the compounds pyrrole[1,2-a]pyrazine-1,4-dione, hexahydro-3-(2-methylpropyl), indole, and phenylpropanamide remained in the heavy phase of extraction (phosphoric acid) and, therefore, were not identified in the samples after extraction, as shown in Fig. 2a.

It was moreover observed that the compounds that remained in the heavy phase are heterocyclic compounds, while those present in the light phase are linear. This fact occurs possibly because the heterocyclic compounds were protonated with the addition of phosphoric acid and become insoluble in organic solvents since they are weak bases. Two linear nitrogenous compounds (hexadecanenitrile and octadecanamide) that remained in the light phase (dichloromethane solvent) also are weak bases, since nitrile and amide groups are present in these molecules. However, compared to the heterocyclic compounds they have longer carbon chains (C16–C18) which can contribute with a better interaction with the organic solvent since long carbon chains have good solubility in organic solvents. Thus, the use of phosphoric acid in extraction proved to be a potential route to separate the nitrogenous compounds in a relatively selective way. The mechanism of interaction of the solvent and heavy phase is most clearly observed by analyzing the FTIR spectra (Section 3.5).

It was observed that some valuable compounds remain in heavy phase such as the Pyrrole [1,2-a] pyrazine-1, 4-dione, hexahydro-3-(2-methylpropyl) (PPDHMP). This compound has been researched by the medical field as a potential compound for cancer treatment and other diseases. Lalitha et al. (2016) studied the potential of PPDHMP, extracted from the marine bacteria *Staphylococcus sp.* strain MB30, in the treatment of lung and cervical cancer. The results show anticancer potential and efficient results in reducing invasions and migrations of cancer cells. Manimaran and Kannabiran (2017) show PPDHMP as a nontoxic potential antioxidant agent for free radicals, which is responsible for the development of cardiovascular, inflammatory diseases, atherosclerosis, cancer, and others.

Octadecanamide is an intermediate compound of relevant industrial interest for the synthesis of other compounds with higher added-value. For example, 100 mg of N-(2-naphthyl) octadecanamide costs currently

on the market \$USD139.00 (MERCK, 2020). Besides, the octadecanamide has been studied by pharmaceutical scientists due to its hypolipidemic activities (ability to reduce blood lipids, lowering cholesterol and consequently cardiovascular risk), for having endogenous mechanisms that influence the desire to sleep, and antidepressant properties (Cheng et al., 2010).

It is worth mentioning that despite the phosphoric acid having preliminarily separated some compounds, further investigations should be carried out in order to purify these components.

3.4.2. Adsorption

Fig. 2.b shows that the activated carbon (SAAC) had satisfactory adsorption results, but there was no selectivity among the compounds. All nitrogenous compounds were adsorbed in higher or lesser percentages. Probably, the sp^3 configuration of nitrogen, in most of these compounds, allows the rotation of the molecules, which enabling higher polar interactions between nitrogen and the activated carbon surface. On this surface, groups SO_3H and SH can be found, due to oxidation with H_2SO_4 (Gomes et al., 2010). Thus, probably the molecules were attracted to the active centers of the SAAC and formed a monolayer.

The nitrogenous compound indole was highly adsorbed, possibly due to H-bonding between the O of SAAC and the H of indol (the two $S=O$ bonds of sulfuric acid make the SAAC operate as a good receptor for the H-bond). Moreover, the numbers of C (sp^2), high ionization and charge on the nitrogen atom from indole may have contributed to higher the forces of attraction between it and the adsorbent (Li et al., 2019a). The adsorbent showed less selectivity with the nitrogenous compounds octadecanamide and hexadecanenitrile. These two compounds are larger molecules ($C_{18}H_{37}NO$ and $C_{16}H_{31}N$) compared to the other compounds studied, which increased their difficulty of being adsorbed on the active sites of activated carbon. Thus, it can be inferred that the texture characteristics of the adsorbent SAAC (surface area $492.9\text{ m}^2\text{ g}^{-1}$ and pore diameter 37.4 \AA) (Ferreira et al., 2019) are favorable to the adsorption of smaller molecules.

Concerning the other compounds present in the bio-oil, the compounds amylene hydrate, trichloromethane, and butane, 2-chloro-2-methyl were absorbed in their entirety, probably due to the chemical bonds between the Cl and O elements, present in these compounds, and the sulfur groups of the SAAC surface. Heptadecane, however, was less adsorbed, probably because it has a larger carbon chain ($C_{17}H_{36}$) and does not have a heteroatom in its structure, thus making difficult the chemisorption.

In agreement with this work, Li et al. (2019b) observed that the adsorption of nitrogenous compounds with activated carbon does not have selectivity. Bhadra and Jung (2020) reported better results in removing nitrogenous compounds in bio-oil using a metal-organic framework adsorbent than activated carbon. For both works, the focus was the removal of nitrogenous compounds as a way of purifying the bio-oil for its use as a fuel. Thus, the selectivity of the adsorption among the nitrogenous compounds was not a relevant fact.

It is worth mentioning that the adsorption technique for the separation of nitrogenous compounds is promising, but in the case of fine chemistry, it requires a more in-depth study. It should find adsorbents with polarities closer to the adsorbates and also choose materials without chemical treatment, so it is possible to obtain a desorption of the products of interest.

3.5. Fourier transform infrared (FTIR) analysis

The FTIR spectra of the bio-oil, produced by pyrolysis under the test 13 conditions for the formation of the nitrogenous compounds, and the two extraction phases (light and heavy phases) were recorded over the $400\text{--}4000\text{ cm}^{-1}$ region. The bio-oil samples (before and after extraction) have almost the same functional groups, except for the heavy phase, which has differences in absorbance peak.

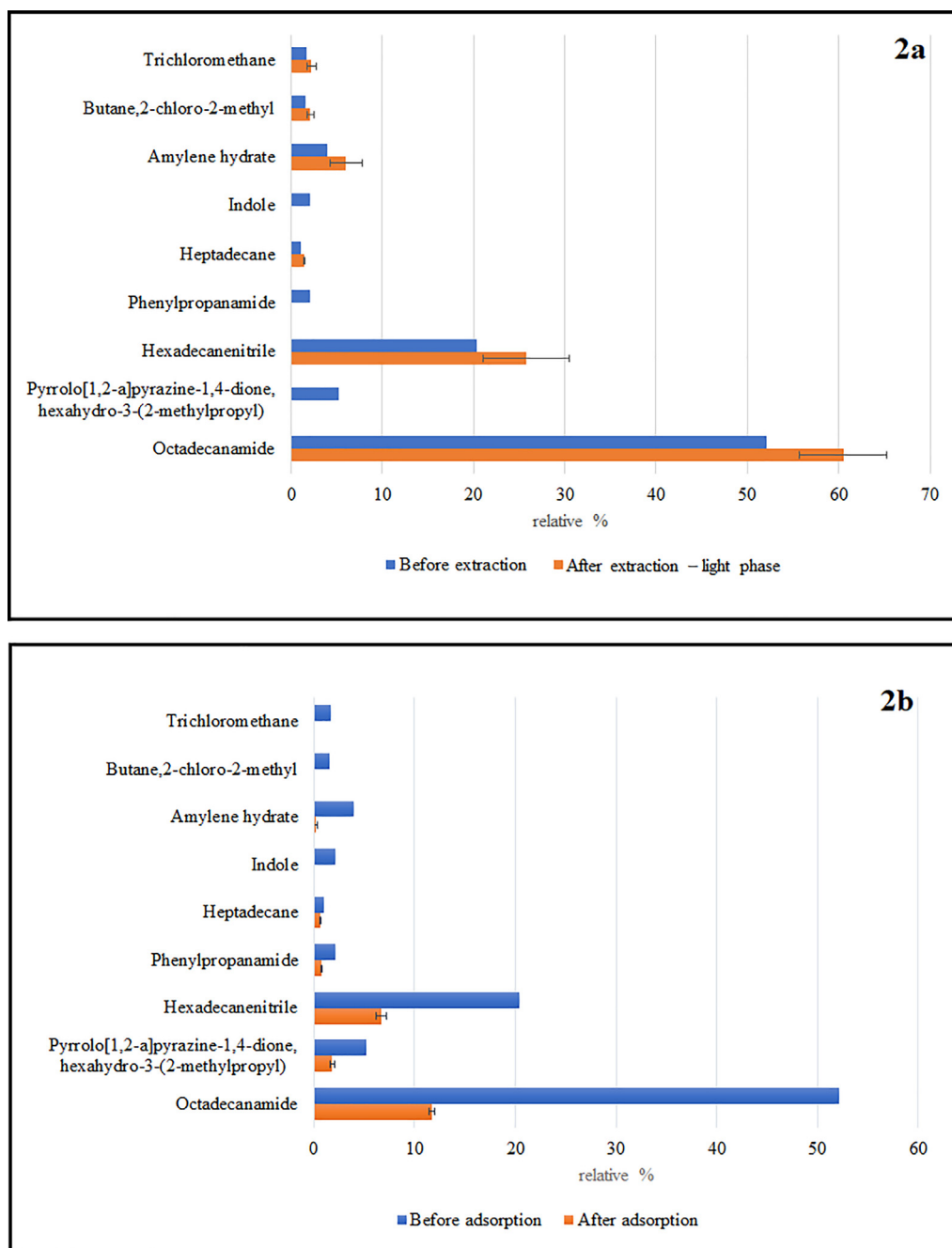


Fig. 2. 2a Results of GC–MS analysis for before and after extraction with phosphoric acid. 2b Results of GC–MS analysis for before and after adsorption.

A broad absorption band between 3700 and 3000 cm^{-1} was observed, which was associated with O–H stretching vibrations, demonstrating the presence of oxygenated compounds in the bio-oil (Aboulkas et al., 2017). The N–H vibrations, associated with nitrogenous compounds, are found in the bands over 3300 cm^{-1} which overlaps the vibrations of the O–H. A weak absorption band located around 2900 cm^{-1} indicated the presence of C–H bending vibrations and suggested the presence of hydrocarbons. The strong absorption band around 1600 cm^{-1} indicated the presence of functional groups C=O, C=C, and C=N that could be associated with carboxylic acids, esters, and aryl ketones (Andrade et al., 2018; Jena and Das, 2011). The absorbance peak around $800\text{--}600\text{ cm}^{-1}$ was associated with aromatics compounds (Francavilla et al., 2015).

The distinct peaks in the light and heavy phase evidence the interaction between the phosphoric acid and the heavy phase compounds.

This interaction leads to a spectral modification, in particular in the regions $2800\text{--}2000\text{ cm}^{-1}$ and $1300\text{--}400\text{ cm}^{-1}$. It is possible to notice that in the high-frequency region ($\approx 3500\text{ cm}^{-1}$) the intensity of bands assigned above to free and hydrogen bonded NH groups diminishes with the addition of H_3PO_4 , before becoming masked by the strong absorption $\nu(\text{OH})$ (Glipta et al., 1999). The broad weak bands that appear around $2800\text{--}2000\text{ cm}^{-1}$ indicate the formation of strong hydrogen bonds between NH groups, H_2PO_4^- ions, and H_3PO_4 (Pu et al., 2005). The phosphoric acid also induces an increase in the intensity of band 1645 cm^{-1} , which is known to be sensitive to protonation (Bouchet and Siebert, 1999). This region could be attributed to a rings vibration and the protonation could be occurring in imide or imino nitrogen group (Foglizzo and Novak 1969; Pu et al., 2005). The increase of 1645 cm^{-1} peak probably occurs due to raising of electron density on carbon of the heterocycle when the imide or imino is protonated,

leading to an increase in absorption frequencies vibrations of some rings (ν (C–N) (Bouchet and Siebert, 1999). The change in the shape of absorption bands in the lower frequency regions $1300\text{--}400\text{ cm}^{-1}$ indicates the presence of characteristic phosphoric anions such as H_2PO_4^- and HPO_4^{2-} (Pu et al., 2005), which reinforces the interaction of phosphoric acid with heavy phase.

It is noteworthy that the bio-oil produced by pyrolysis, is a complex mixture of compounds. Thus, the improvement of separation methods (adsorption or extraction) it would be possible to use more accurate quantitative methods for measuring the compounds.

4. Conclusion

The operational parameters of slow pyrolysis *Spirulina platensis* for improved liquid yield and production of nitrogenous compounds, for fine chemistry application, was evaluated. For this purpose, CCD and an optimization technique were used. Also, adsorption and extraction were investigated as separation routes. The effect temperature and heating rate was the most significant on liquid yield. The optimization study determined 1.98 g , $556\text{ }^\circ\text{C}$, and $10.24\text{ }^\circ\text{C min}^{-1}$ to maximize liquid yield. Semi-quantitative GC–MS analysis revealed a high concentration of nitrogenous compounds in liquid fraction. The extraction and adsorption showed promising for purification of nitrogenous compounds; however, further investigations must be realized.

Declaration of interests

The authors declare that they have no known competing financial interests or personal relationships that could have appeared to influence the work reported in this paper.

CRediT authorship contribution statement

K.C. Rocha: Formal analysis, Investigation, Writing - original draft, Validation, Visualization. **C.G. Alonso:** Resources, Writing - review & editing. **W.G.O. Leal:** Investigation, Resources, Formal analysis. **E.L. Schultz:** Resources, Writing - review & editing. **L.A. Andrade:** Conceptualization, Methodology, Formal analysis, Writing - original draft, Supervision, Project administration. **I.C. Ostroski:** Conceptualization, Methodology, Writing - original draft, Supervision, Project administration, Funding acquisition.

Acknowledgements

This study was financed by the Coordenação de Aperfeiçoamento de Pessoal de Nível Superior – Brasil (CAPES) – Finance Code 001.

Appendix A. Supplementary data

Supplementary data to this article can be found online at <https://doi.org/10.1016/j.biortech.2020.123709>.

References

Aboulkas, A., Hammani, H., El Achaby, M., Bilal, E., Barakat, A., El harfi, K., 2017. Valorization of algal waste via pyrolysis in a fixed-bed reactor: production and characterization of bio-oil and bio-char. *Bioresour. Technol.* 243, 400–408. <https://doi.org/10.1016/j.biortech.2017.06.098>.

Akhtar, J., Noraishah, S.A., 2012. A review on operating parameters for optimum liquid oil yield in biomass pyrolysis. *Renew. Sustain. Energy Rev.* 16, 5101–5109. <https://doi.org/10.1016/j.rser.2012.05.033>.

Andrade, L.A., Barrozo, M.A.S., Vieira, L.G.M., 2018. Catalytic solar pyrolysis of microalgae *Chlamydomonas reinhardtii*. *Sol. Energy* 173, 928–938. <https://doi.org/10.1016/j.solener.2018.08.035>.

Ataefard, M., Saeb, M.R., 2015. A multiple process optimization strategy for manufacturing environmentally friendly printing toners. *J. Clean. Prod.* 108, 121–130. <https://doi.org/10.1016/j.jclepro.2015.07.016>.

Ataefard, M., Shadman, A., Saeb, M.R., Mohammadi, Y., 2016. A hybrid mathematical model for controlling particle size, particle size distribution, and color properties of

toner particles. *Appl. Phys. A Mater. Sci. Process.* 122, 1–14. <https://doi.org/10.1007/s00339-016-0242-1>.

Barbosa, J.M., Andrade, L.A., Vieira, L.G.M., Barrozo, M.A.S., 2020. Multi-response optimization of bio-oil production from catalytic solar pyrolysis of *Spirulina platensis*. *J. Energy Inst.* <https://doi.org/10.1016/j.joei.2019.12.001>.

Bhadra, B.N., Jhung, S.H., 2020. Adsorptive removal of nitrogenous compounds from microalgae-derived bio-oil using metal-organic frameworks with an amino group. *Chem. Eng. J.* 388, 124195. <https://doi.org/10.1016/j.cej.2020.124195>.

Bouchet, R., Siebert, E., 1999. Proton conduction in acid doped polybenzimidazole. *Solid State Ionics* 118, 287–299.

Bridgwater, A.V., Bridge, S.A., 1991. A review of biomass pyrolysis and pyrolysis technologies. *Biomass Pyrol. Liq. Upgrad. Util.* 11–92. https://doi.org/10.1007/978-94-011-3844-4_2.

Cheng, M.C., Ker, Y., Yu, T.H., Lin, L.Y., Peng, R., Peng, C.H., 2010. Chemical synthesis of 9 (Z)-octadecenamide and its hypolipidemic effect : a bioactive agent found in the essential oil of mountain celery seeds 9, 1502–1508. <https://doi.org/10.1021/jf903573g>.

Fan, Y., Cai, D., Zhang, S., Wang, H., Guo, K., Zhang, L., Yang, L., 2019. Effective removal of nitrogen compounds from model diesel fuel by easy-to-prepare ionic liquids. *Sep. Purif. Technol.* 222, 92–98. <https://doi.org/10.1016/j.seppur.2019.04.026>.

Fanghua, L., Srivatsa, S.C., Bhattacharya, S., 2019. A review on catalytic pyrolysis of microalgae to high-quality bio-oil with low oxygenous and nitrogenous compounds. *Renew. Sustain. Energy Rev.* 108, 481–497. <https://doi.org/10.1016/j.rser.2019.03.026>.

Fermoso, J., Coronado, J.M., Serrano, D.P., Pizarro, P., 2017. Pyrolysis of microalgae for fuel production. *Microalgae-Based Biofuels and Bioproducts*. Elsevier Ltd. <https://doi.org/10.1016/B978-0-08-101023-5.00011-X>.

Ferreira, M.E., Vaz, B.G., Borba, C.E., Alonso, C.G., Ostroski, I., 2019. Modified activated carbon as a promising adsorbent for quinoline removal. *Micropor. Mesopor. Mater.* <https://doi.org/10.1016/j.micromeso.2018.10.034>.

Francavilla, M., Manara, P., Kamaterou, P., Monteleone, M., Zabanitout, A., 2015. Cascade approach of red macroalgae *Gracilaria gracilis* sustainable valorization by extraction of phycobiliproteins and pyrolysis of residue. *Bioresour. Technol.* 184, 305–313. <https://doi.org/10.1016/j.biortech.2014.10.147>.

Foglizzo, R., Novak, A., 1969. Spectres de vibration de quelques halogénures de pyridinium. *J. Chim. Phys.* 66, 1539–1550. <https://doi.org/10.1051/jcp/196966s21539>.

Glipa, X., Bonnet, B., Mula, B., Jones, D.J., Rozière, J., 1999. Investigation of the conduction properties of phosphoric and sulfuric acid doped polybenzimidazole. *J. Mater. Chem.* 9, 3045–3049. <https://doi.org/10.1039/a906060j>.

Gomes, H.T., Miranda, S.M., Sampaio, M.J., Silva, A.M.T., Faria, J.L., 2010. Activated carbons treated with sulphuric acid: catalysts for catalytic wet peroxide oxidation. *Catal. Today* 151, 153–158. <https://doi.org/10.1016/j.cattod.2010.01.017>.

Guedes, R.E., Luna, A.S., Torres, A.R., 2018. Operating parameters for bio-oil production in biomass pyrolysis: a review. *J. Anal. Appl. Pyrol.* 129, 134–149. <https://doi.org/10.1016/j.jaap.2017.11.019>.

Guo, F., Wang, X., Yang, X., 2017. Potential pyrolysis pathway assessment for microalgae-based aviation fuel based on energy conversion efficiency and life cycle. *Energy Convers. Manag.* 132, 272–280. <https://doi.org/10.1016/j.enconman.2016.11.020>.

Han, D.Y., Li, G.X., Cao, Z.B., Zhai, X.Y., Yuan, M.M., 2013. A study on the denitrogenation of Fushun shale oil. *Energy Sour. Part A* 622–628. <https://doi.org/10.1080/15567036.2010.509085>.

Hong, Y., Chen, W., Luo, X., Pang, C., Lester, E., Wu, T., 2017. Microwave-enhanced pyrolysis of macroalgae and microalgae for syngas production. *Bioresour. Technol.* 237, 47–56. <https://doi.org/10.1016/j.biortech.2017.02.006>.

Hosseinnezhad, M., Shadman, A., Saeb, M.R., Mohammadi, Y., 2017. A new direction in design and manufacture of co-sensitized dye solar cells: toward concurrent optimization of power conversion efficiency and durability. *Opto-Electron. Rev.* 25, 229–237. <https://doi.org/10.1016/j.opelre.2017.06.003>.

Hu, X., Gholizadeh, M., 2019. Biomass pyrolysis: a review of the process development and challenges from initial researches up to the commercialisation stage. *J. Energy Chem. Elsevier B.V. and Science Press.* <https://doi.org/10.1016/j.jechem.2019.01.024>.

Hu, Z., Zheng, Y., Yan, F., Xiao, B., Liu, S., 2013. Bio-oil production through pyrolysis of blue-green algae blooms (BGAB): product distribution and bio-oil characterization. *Energy* 52, 119–125. <https://doi.org/10.1016/j.energy.2013.01.059>.

Huang, F., Tahmasebi, A., Maliutina, K., Yu, J., 2017. Formation of nitrogen-containing compounds during microwave pyrolysis of microalgae: product distribution and reaction pathways. *Bioresour. Technol.* 245, 1067–1074. <https://doi.org/10.1016/j.biortech.2017.08.093>.

Jena, U., Das, K.C., 2011. Comparative evaluation of thermochemical liquefaction and pyrolysis for bio-oil production from microalgae. *Energy Fuels* 25, 5472–5482. <https://doi.org/10.1021/ef201373m>.

Lalitha, P., Veena, V., Vidhyapriya, P., Lakshmi, Pragna, Krishna, R., Sakthivel, N., 2016. Anticancer potential of pyrrole (1, 2, 4) pyrazine 1, 4, dione, hexahydro 3-(2-methyl propyl) (PPDHMP) extracted from a new marine bacterium, *Staphylococcus* sp. strain MB30. *Apoptosis* 21 (5), 566–577. <https://doi.org/10.1007/s10495-016-1221-x>.

Li, F., Katz, L., Hu, Z., 2019a. Adsorption of major nitrogen-containing components in microalgal bio-oil by activated carbon: equilibrium, kinetics, and ideal adsorbed solution theory (IAST) model. <https://doi.org/10.1021/acsuschemeng.9b03804>.

Li, F., Katz, L., Qiu, S., 2019b. Adsorptive selectivity and mechanism of three different adsorbents for nitrogenous compounds removal from microalgae bio-oil. *Ind. Eng. Chem. Res.* 58, 3959–3968. <https://doi.org/10.1021/acs.iecr.8b04934>.

Ma, Z., Zhang, Y., Li, C., Yang, Y., Zhang, W., Zhao, C., Wang, S., 2019. N-doping of biomass by ammonia (NH₃) torrefaction pretreatment for the production of renewable N-containing chemicals by fast pyrolysis. *Bioresour. Technol.* 292, 122034. <https://doi.org/10.1016/j.biortech.2019.122034>.

- Maliutina, K., Tahmasebi, A., Yu, J., 2018. The transformation of nitrogen during pressurized entrained-flow pyrolysis of *Chlorella vulgaris*. *Bioresour. Technol.* 262, 90–97. <https://doi.org/10.1016/j.biortech.2018.04.073>.
- Manimaran, M., Kannabiran, K., 2017. Marine *Streptomyces* Sp. VITMK1 derived pyrrolo [1, 2-A] pyrazine-1, 4-dione, hexahydro-3-(2-methylpropyl) and its free radical scavenging activity. *Open Bioact. Compd. J.* 23–30. <https://doi.org/10.2174/1874847301705010023>.
- MERCK. Chemicals catalog, 2020. < <https://www.sigmaaldrich.com/catalog/product> > . Accessed on: 16 April 2020.
- Pourkarimi, S., Hallajisani, A., Alizadehdakhel, A., Nouralishahi, A., 2019. Biofuel production through micro- and macroalgae pyrolysis – a review of pyrolysis methods and process parameters. *J. Anal. Appl. Pyrol.* 104599. <https://doi.org/10.1016/j.jaap.2019.04.015>.
- Pu, H.T., Qiao, L., Liu, Q.Z., Yang, Z.L., 2005. A new anhydrous proton conducting material based on phosphoric acid doped polyimide. *Eur. Polym. J.* 41, 2505–2510. <https://doi.org/10.1016/j.eurpolymj.2005.04.033>.
- Qiang, L., Wen-zhi, L., Dong, Z., Xi-feng, Z., 2009. Analytical pyrolysis-gas chromatography/mass spectrometry (Py-GC/MS) of sawdust with Al/SBA-15 catalysts. *J. Anal. Appl. Pyrol.* 84, 131–138. <https://doi.org/10.1016/j.jaap.2009.01.002>.
- Salleh, M., Hadj-kali, M., Hizaddin, H., Hashim, M., 2017. Extraction of nitrogen compounds from model fuel using 1-ethyl-3-methylimidazolium methanesulfonate. *Sep. Purif. Technol.* <https://doi.org/10.1016/j.seppur.2017.07.068>.
- Sharma, A., Wang, S., Pareek, V., Yang, H., Zhang, D., 2015. Multi-fluid reactive modeling of fluidized bed pyrolysis process. *Chem. Eng. Sci.* 123, 311–321. <https://doi.org/10.1016/j.ces.2014.11.019>.
- Simão, B.L., Santana, J.A., Chagas, B.M.E., Cardoso, C.R., Ataíde, C.H., 2018. Pyrolysis of *Spirulina maxima*: kinetic modeling and selectivity for aromatic hydrocarbons. *Algal Res.* 32, 221–232. <https://doi.org/10.1016/j.algal.2018.04.007>.
- Smith, R.H., 1981. Denitrogenation of oils with reduced hydrogen consumption. U.S. Patent No 4,261,813.
- Vieira, L.G.M., Silvério, B.C., Damasceno, J.R., Barrozo, M.A.S., 2011. Performance of hydrocyclones with different geometries 89, 655–662. <https://doi.org/10.1002/cjce.20461>.
- Wang, X., Tang, X., Yang, X., 2017. Pyrolysis mechanism of microalgae *Nannochloropsis* sp. based on model compounds and their interaction. *Energy Convers. Manag.* 140, 203–210. <https://doi.org/10.1016/j.enconman.2017.02.058>.
- Yang, X., Wang, X., Zhao, B., Li, Y., 2014. Simulation model of pyrolysis biofuel yield based on algal components and pyrolysis kinetics. *Bioenergy Res.* 7, 1293–1304. <https://doi.org/10.1007/s12155-014-9467-z>.